Segmentation of lung fields in digital chest radiographs by artificial neural networks

G. Coppini, M. Paterni, L. Guerriero, E.M. Ferdeghini
CNR Institute of Clinical Physiology, Pisa, Italy

INTRODUCTION

The diffusion of digital radiography has greatly enhanced the potential for computational analysis of chest images [1]. Various problems such as lung nodule detection [2], analysis of lung parenchyma alterations [1], description of the lung shape for emphysema assessment [3] have been investigated. Lung field segmentation is a basic step for virtually any quantitative procedure. In this view, due to the imaging process and the complexity of the imaged district, an efficient use of prior anatomical knowledge is crucial. In this report we describe a new approach to lung field segmentation which is based on fuzzy boundary modeling and a neural network architecture including supervised multilayer networks and topology preserving maps.

METHODS

Let us consider curve defined by the lung field boundary (LFB): we use it as the centerline of a Gaussian membership function that identifies a fuzzy set of lung boundary points. Given a radiogram, the segmentation goal is then referred back to computing the membership function from image features. According to boundary-based segmentation approaches, differential features look well suited for such a task. Using a properly labeled training set, a neural network of the feed-forward type is trained to learn the membership from differential feature at position (x, y). Afterwards, the wanted LFB is obtained by defuzzification of the fuzzy boundary. To this end the regularized ridge of the membership function is computed by the relaxation of a 1D Topology Preserving Map (TPM) network ($n=40$ units). As we look for a closed curve, the units are arranged into a circle so that the network is topologically equivalent to the boundary of interest. Each unit in the TPM has a 2D weight vector $\mathbf{w} = (w_x, w_y)$ representing image plane coordinates. At time t of relaxation phase the point $\mathbf{x}(t)$ is randomly selected in the image plane and used to feed the network. The following modified update rule is used:

$$c = \arg\min_i \{\| \mathbf{x}(t) - \mathbf{w}_i \|\}$$

$$\mathbf{w}_j(t) = \mathbf{w}(t-1) + \alpha(t) G(j,c) l(x,y) \| \mathbf{x}(t) - \mathbf{w}_j(t-1) \|$$

where $\alpha(t)$ is a linearly decreasing gain, $G(j,c)$ is a Gaussian neighborhood function with a standard deviation $\sigma(t)$ (linearly decreasing in time). As one expects that lung boundaries correspond to high $l(x,y)$ values, we added the factor $l(x,y)$ in the weight adaptation rule so as to drive the network weights into image points corresponding to $l(x,y)$ maxima. In Figure 1c we show the final boundary.

To test the method, a dataset including 189 cases was employed. For each case, postero-anterior and lateral digital chest radiographs (Thorax 2000, IMIX, Finland) were obtained: radiographs were 2000×2000 pixels ($198\ \mu m$ per pixel), with a dynamic range of 12 bits. In each image, expert physicians outlined the boundary of the lung fields. Each picture $I(x,y)$ is processed as follows:

1) Normalization. This step is aimed to obtain (approximate) scale invariance. A bounding box is identified by grey-level profiles in vertical and horizontal directions respectively. The image is rescaled with bilinear interpolation so as the bounding box fits a rectangle with a prefixed size.
2) Edge feature computation. In this phase, following Gaussian filtering, the magnitude of the gradient $|\nabla I(x,y)|$ and the Laplacian $\nabla^2 I(x,y)$ of the normalized radiograph are computed.
3) Pattern extraction. For each lung boundary, a set of *2000* points is randomly extracted form the radiogram with the constraint that *1000* of them lie in the boundary strip, and the remaining are outside. Thus, we obtain *2000* training patterns:

$$[|\nabla I(x,y)|, \nabla^2 I(x,y), x, y]$$

The coordinates (x, y) are explicitly included so as to account for the space varying nature of the membership. A subset of the entire dataset including 64 randomly chosen cases was utilized to train three neural networks: two of them compute the membership function in postero-anterior view for right and left lung, respectivley, and the remaining processes the lateral view. Each network has four input units, one hidden layer with 25 units (experiments with more hidden units did not provided significant improvements), and a single output unit whose

activation value estimates $l(x,y)$. Standard error back-propagation rule with momentum term was used for training. Once the networks are trained, images are processed according to steps 1 and 2 as in the training phase and $l(x,y)$ is computed. An example of estimated lung boundary membership is shown in Figure 1b.

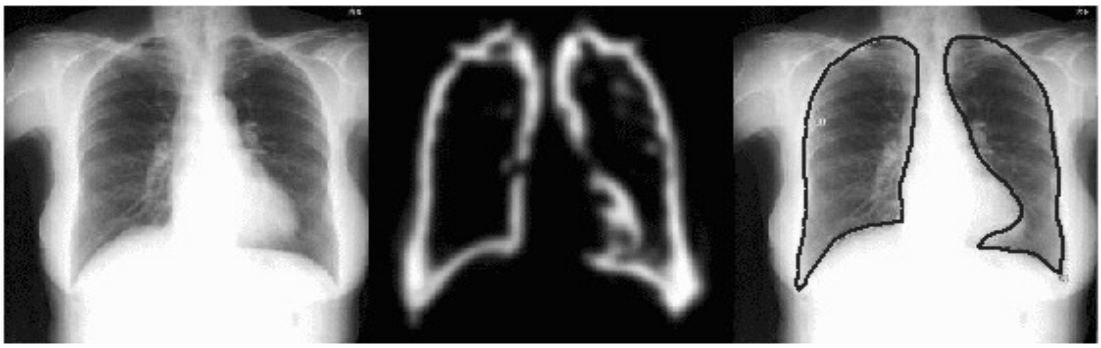

a) b) c)

Figure 1. a) Postero-anterior radiogram; b) estimated lung boundary memberships; c) lung boundary obtained from the membership in panel b).

RESULTS AND DISCUSSION

We have tested the method on the cases of the dataset not included in the training set (*N=125*). Comparison of the segmentation with the boundary traced by the physician was performed. Let A^r be the area enclosed by the traced contour, A^c the area of the region simultaneously enclosed by the computed contour and the traced one, A^+ the area enclosed by the computed contour whose points are outside the traced region, and A^- the area of the region inside the traced contour but not included in the computed one. The following quantities are then evaluated:

$TP = A^c / A^r \qquad FP = A^+ / A^r, \qquad FN = A^- / A^r.$

The related average values are shown in Table I.

Contour	*TP*	*FP*	*FN*
Right lung in postero-anterior view	$97.5\% \pm 2.3$	$3.5\% \pm 2.1$	$2.8\% \pm 2.5$
Left lung in postero-anterior view	$96.4\% \pm 2.5$	$2.7\% \pm 1.9$	$3.2\% \pm 2.5$
Lung zone in lateral view	$97.1\% \pm 2.4$	$8.2\% \pm 2.9$	$3.9\% \pm 3.6$

Table I. Performances of the segmentation method. Average values plus/minus standard deviation.

Experimental results support the idea that neural networks are well suited to exploit prior knowledge about the shape and location of lung boundaries in chest radiographs. Interestingly, the proposed method behaves reasonably well also in lateral views whose quality is usually very poor. Actually, in lateral projections lung boundaries are usually poorly defined due object thickness and overlapping of imaged structures.

REFERENCES

[1] B. van Ginneken, B.M: ter Haar Romeny, M. Viergever. Computer-aided diagnosis in chest radiography: a survey. IEEE Trans Med Imaging 20:1228–41, 2001.

[2] G. Coppini, S. Diciotti, M. Falchini, N. Villari, G. Valli. Neural networks for computer-aided diagnosis: detection of lung nodules in chest radiograms. IEEE Transactions on Information Technology in Medicine, 7:344–57, 2003.

[3] G. Coppini, M. Miniati, M. Paterni, S. Monti, E.M. Ferdeghini. Computer-aided diagnosis of emphysema in COPD patients: Neural-network-based analysis of lung shape in digital chest radiographs. Medical Engineering & Physics, 29 :76–86, 2007.